Corrosion Behavior of Zinc Cold Spray Coatings (ZnCr & ZnNb) in a Simulated Natural Gas Environment Containing H_2O, CO_2, and H_2S

Zineb Belarbi
National Energy Technology Laboratory
1450 Queen Avenue SW
Albany, OR 97321
USA
NETL Support Contractor
1450 Queen Avenue SW
Albany, OR 97321
USA

Richard E. Chinn
National Energy Technology Laboratory
1450 Queen Avenue SW
Albany, OR 97321
USA

Ömer N. Doğan
National Energy Technology Laboratory
1450 Queen Avenue SW
Albany, OR 97321
USA

ABSTRACT

The natural gas transmission pipeline network in the U.S. consists of approximately 300,000 miles, is made mainly of carbon steel, and was installed in the 1950s and 1960s. Understanding the pipeline steel behavior in natural gas will inform new pipeline designs and repurposing of existing pipelines. Sulfide stress cracking (SSC) is a problem for steel pipelines transporting natural gas or CO_2 containing partial pressures of H_2S higher than 0.3 kPa (0.05 psi). Therefore, the objective of this work is to mitigate internal corrosion in steel pipelines transporting natural gas containing H_2S using cold spray coatings. Two types of the cold spray binary metallic coatings (zinc chromium (ZnCr), zinc niobium (ZnNb)) were studied using electrochemical techniques: potentiodynamic polarization (PDP), linear polarization resistance (LPR), and electrochemical impedance spectroscopy (EIS). The evaluation of the corrosion resistance of cold spray coatings (ZnCr, ZnNb) was carried out in an environment containing 3 barg CO_2 pressure, simulating the partial pressures that are found in gas transmission over a solution of 3.5 wt.% NaCl heated to 40 °C. To simulate sour conditions, a concentration of 0.003 M $Na_2S_2O_3.5H_2O$, which corresponds to H_2S partial pressures around 0.079 bar (1.146 psi), was used. Post-corrosion surface characterization was performed using a scanning electron microscopy (SEM) equipped with energy-dispersive X-ray spectroscopy (EDS) and X-ray diffraction analysis (XRD). The obtained data showed that the presence of 0.003 M $Na_2S_2O_3.5H_2O$ shifted the corrosion potential to more anodic potential and decreased the corrosion current density. The tested coatings showed similar behavior after 1 hour of exposure in CO_2/H_2S environment, which indicated that similar electrochemical reactions were taking place on ZnNb and ZnCr. SEM images and EDS surface analyses for specimens showed a significant change in surface chemical composition of carbon steel coated with ZnNb and ZnCr, after 24 hours of immersion in 3.5

wt.% NaCl solution saturated with CO_2 containing 0.003 $Na_2S_2O_3.5H_2O$ at 40 °C. No localized attack was observed. The EDS mapping analysis and XRD results revealed the presence of zinc sulfide (ZnS).

Key words: CO_2 corrosion, natural gas pipelines, cold spray coatings, zinc alloy, sacrificial coatings, self-healing coatings, electrochemical reaction autoclave, zinc sulfide

INTRODUCTION

Hydrogen sulfide promotes corrosion of carbon steels and hydrogen embrittlement by increasing the adsorption of atomic hydrogen produced by the internal corrosion of steel pipelines [1, 2]. Internal corrosion in natural gas pipelines is primarily caused by the presence of carbon dioxide (CO_2), hydrogen sulfide (H_2S), and if ingress occurs oxygen (O_2) dissolved in the small amount of incidental water such as the mist carryover after the gas dehydration process [3]. Several studies have shown that the presence of H_2S concentrations below 690 Pa could cause the formation of a protective iron sulfide film [4, 5, 6]. Ma et al. [7] showed that the presence of H_2S at concentrations lower than 0.04 mmol dm^{-3}, at pH value of 3–5, and longer immersion time (≥ 2 hours) cause an inhibition of the corrosion of carbon steel. The inhibition effect of H_2S could be due to the formation of iron sulfide with different crystal structures, such as amorphous ferrous sulfide, mackinawite, cubic ferrous sulfide, smythite, greigite, pyrrhotite, troilite, and pyrite [8, 9, 10]. Choi et al. [10] evaluated the effect of very low-level H_2S on CO_2 corrosion of carbon steel in 1 wt.% NaCl solution (25 °C) at pH of 3 and 4, and under atmospheric pressure, and investigated the mechanism of the iron sulfide layer formation. The results obtained by Choi et al. [10] showed that the addition of 100 ppm H_2S to CO_2 led to the formation of an iron sulfide layer which reduced the corrosion rate of carbon steel in CO_2/H_2S environments. The author claimed that the formation of thin FeS film (tarnish) on the steel surface suppressed the anodic dissolution reaction. Sulfide stress cracking (SSC) is a problem for steel pipeline transporting natural gas containing partial pressures of H_2S higher than 0.3 kPa (0.05 psi) [11].

In situ pH and H_2S partial pressure are considered to define regions with different severity with respect to the SSC of carbon and low-alloy steels (Figure 1) [12]. The presence of H_2S and CO_2 in the gas phase lowers the pH of the environment below the de-passivation pH of the steel alloy, increasing the rate of proton release. Localized corrosion can be a precursor for SSC due to de-passivation inside pits and crevices [13]. SSC and internal corrosion of steel pipelines can cause natural gas leakage, leading to wasted energy, explosion hazards, and methane emissions.

To protect natural gas transmission pipelines and equipment from internal corrosion, cold spray metallic coatings can be used. Cold sprayed zinc (Zn) coatings are mainly used as sacrificial coating to protect steel against marine corrosion [14, 15]. Chavan et al. [16] evaluated the effect of heat treatment on corrosion performance of Zn cold sprayed coating deposited on mild steel exposed to atmospheric corrosion. The authors found that Zn coatings provided an excellent corrosion barrier to mild steel exposed to the marine environment. To our knowledge, very little research has been done on using cold spray coating to mitigate CO_2 internal corrosion in natural gas pipelines. This paper is a continuation of work that has been done in a laboratory setting [17]. The corrosion behavior of zinc chromium (ZnCr) and zinc niobium (ZnNb) have been tested in the laboratory [18, 19] and in a live natural gas pipeline at the Northwest Natural gas storage facility in Mist, Oregon [20] under stagnant and flow conditions. The laboratory and the field-test results confirm that the cold spray coatings (ZnCr & ZnNb) provide corrosion protection of carbon steel exposed to wet natural gas under stagnant and flow conditions.

For our study, $Na_2S_2O_3.5H_2O$ has been used as a replacement of H_2S gas. The possibility of replacing H_2S with thiosulfate ($S_2O_3^{2-}$), a non-toxic anion, for studying corrosion of stainless and carbon steels in sour gas conditions was first proposed by Tsujikawa in 1993 [21]. Thiosulfate ($S_2O_3^{2-}$) can be used as a substitute of H_2S because it can reduce to H_2S when in contact with carbon steel [22]. Kappes et al. [22], used the kinetics of H_2S evolution to estimate the range of partial pressure of H_2S that can be simulated with thiosulfate solutions. It was determined that acid brines containing 10^{-4} M and 10^{-3} M $S_2O_3^{2-}$ could be used for replacing continuous bubbling of dilute H_2S/N_2 mixtures in tests of degradation of carbon steels, with H_2S partial pressures ranging between 0.03 and 0.56 kPa (0.05 psi to 0.08 psi). It has been shown in literature that iron sulfide or zinc sulfide (ZnS) can form on carbon steel or Zn alloy exposed to thiosulfate containing solution, respectively [21, 22, 23].

The aim of this study is to mitigate internal corrosion in steel pipelines transporting natural gas containing H_2S using cold spray coatings. The corrosion behavior of carbon steel coated with ZnCr and ZnNb cold spray coatings was investigated in 3.5 wt.% NaCl containing 0.003 M $Na_2S_2O_3.5H_2O$ which correspond to H_2S partial pressures around 0.079 bar (1.146 psi).

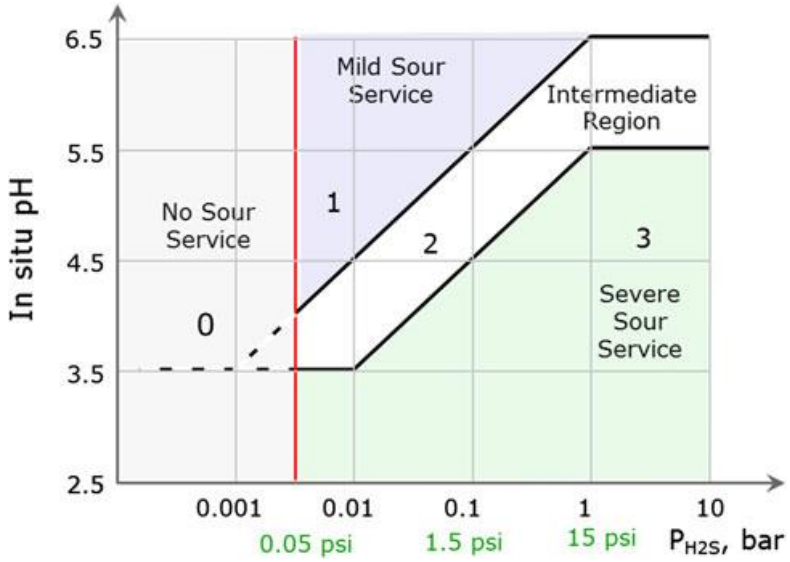

Figure 1: Regions of environmental severity with respect to the SSC of carbon and low-alloy steels [12].

EXPERIMENTAL PROCEDURE

Materials and Chemicals

ZnCr and ZnNb coatings were cold sprayed onto UNS G10180. For confidentiality, the cold spray process conditions will not be presented in this paper. The characteristics of metallic coatings is shown in Table 1. Figure 2 shows the backscattered scanning electron microscopy (SEM) images of the cross-section of UNS G10180 with metallic coatings. SEM images (**Error! Reference source not found.**2) show very dense coating surface with a minimum number of pores. The porosity of cold spray coating was identified by image analysis of the SEM images using ImageJ software. The thickness of the coatings for the ZnCr and ZnNb is 304 µm and 428 µm, respectively. The electrolyte was prepared by dissolving 3.5 g of sodium chloride (NaCl) in 96.5 g of deionized water, which was then saturated with CO_2 by sparging with CO_2. To investigate the effect of impurities such as H_2S on corrosion performance of cold spray coatings, electrochemical measurement was performed in 3.5 wt.% NaCl containing 0.003 M $Na_2S_2O_3.5H_2O$ which correspond to H_2S partial pressures around 0.079 bar (1.146 psi).

Table 1. Characteristics of Metallic Coatings

Coatings	Thickness (µm)	Porosity (%)
ZnCr cold spray coating	304 ± 7.0	≈ 0.5 ± 0.28
ZnNb cold spray coating	428 ± 5.1	≈ 0.32 ± 0.13

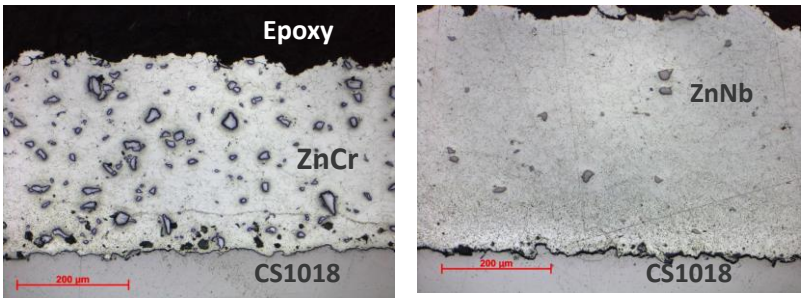

a). CS coated with cold spray coating (ZnCr)

b). CS coated with cold spray coating (ZnNb)

Figure 2: Backscattered SEM micrographs of the cross-section of CS1018 with metallic coatings.

Electrochemical Measurements

To investigate the corrosion behavior of cold spray coatings in simulated field conditions in natural gas transmission pipeline, the corrosion tests were conducted following similar experimental procedures as previous studies [24, 18]. The autoclave made of Hastelloy® C-276 alloy (UNS N10276) with three electrodes configuration setup (Figure) was used to investigate the corrosion behavior of Znx cold spray coatings in simulated natural gas environment containing H_2O, CO_2, and H_2S. Rectangular specimens made of the alloys shown in Table 1 with an exposure of the area of 1 cm^2 (1 cm x 1 cm) were used as working electrodes. Platinum with KCl/AgCl liquid junction and platinum electrodes were used as a reference and counter electrode, respectively. The potential difference between the reference electrode and saturated calomel electrode (SCE) is 48 mV. Therefore, all potentials reported in this study were converted and referred to SCE. Each working electrode was sequentially polished using 400 and 600 grit silicon carbide paper, rinsed with isopropanol in an ultrasonic cleaner for 2 to 3 minutes and air dried, before the immersion in the autoclave. A volume (0.5 L) of 3.5 wt.% NaCl with and without $Na_2S_2O_3.5H_2O$ was introduced in the Teflon™ liner that was placed inside the autoclave vessel heated to 40 °C. To eliminate dissolved oxygen, the solution was sparged with CO_2 for 2 hours.

After the insertion of the sample, the oxygen in the gas phase was removed by pulling the vacuum and back filling with CO_2. This procedure was repeated three times to reduce the residual air in the gas phase. The final pressure of CO_2 in the system was achieved by introducing CO_2 to the liquid phase until pressure become stable (4.08 bar). The pH of the measured pressurized solution was approximately 4 ± 0.1 before and after experiments. Investigation of corrosion behavior of the metallic coating was performed by

electrochemical methods using potentiodynamic polarization (PDP), linear polarization resistance (LPR), and electrochemical impedance spectroscopy (EIS). All electrochemical measurements were conducted after 1 hour of immersion and after a steady open circuit potential (OCP) was reached. Potentiodynamic polarization curves were recorded from -0.2 V vs. OCP up to 1.5 V vs. OCP at a scan rate of 1 mV/s. Resistance of polarization R_p was measured using LPR by polarizing the working electrode from -5 mV to +5 mV vs. OCP; using a scan rate of 0.125 mV/s. The Tafel value (β_a and β_c) for these experiments were determined by Tafel's extrapolation method. The corrosion current I_{corr} was calculated considering the Stern-Geary assumption (Equation 1) [25].

$$I_{corr} = \frac{1}{R_p} * \frac{\beta_a * \beta_c}{2.303(\beta_a + \beta_c)} \quad (1)$$

The corrosion rate was calculated using the following Equation [26]:

$$CR = K * \frac{I_{corr} * EW}{\rho * A} \quad (2)$$

Where *CR* is corrosion rate in mm/y; *K*: conversion factor (3,270 mm. g/A.cm. y); EW: equivalent weight (727.92 g/equivalent for UNS G10180, 29.36 g/equivalent for ZnCr, and 32.64 for ZnNb); *A*: area in cm^2; ρ: density of substrate (7.87 g/cm^3 for UNS G10180, 7.14 g/cm^3 for ZnCr, and 7.18 g/cm^3 for ZnNb); I_{corr}: corrosion current in A. The EIS measurements were carried out over a frequency range of 20 kHz to 10 mHz using an AC amplitude of 10 mV (rms). LPR and EIS data were measured every hour during a total exposure time of 24 hours. Electrochemical measurements were carried out using a Gamry Reference 600+[††1] potentiostat/galvanostat. To verify the reproducibility of the results, all the electrochemical tests were repeated 2 to 3 times. The test matrix is shown in Table 2.

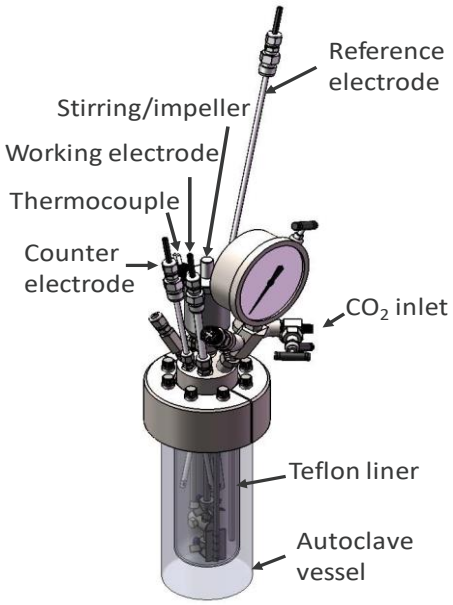

Figure 3: Experimental setup for electrochemical autoclave.

[††] Trade name

Table 2. Experimental Matrix for Electrochemical Tests

Total pressure (bar)	4.08
pCO_2 (bar)	4
Solution	0.5 L of 3.5 wt.% NaCl + 0.003 M $Na_2S_2O_3.5H_2O$
Solution temperature	40 °C
Working electrode	Uncoated carbon steel (UNS G10180) Coated carbon steel with cold spray coating ZnCr Coated carbon steel with cold spray coating ZnNb

Surface Analysis

Typically, after 24 hours of immersion in 3.5 wt.% NaCl saturated with CO_2 containing $Na_2S_2O_3.5H_2O$, the samples were taken out, rinsed with isopropyl alcohol, dried, and the exposed surface was characterized by a SEM (FEI Inspect-F††) and an EDAX energy dispersive X-ray spectroscopy (EDS) system. Imaging was performed at an accelerating voltage of 15 kV using a secondary electron signal (SE) and base scattered electron (BSE) for the cross-section images. Chemical analysis of exposed surface was performed using EDS.

RESULTS

Potentiodynamic Polarization Curve

Figure 4 shows potentiodynamic polarization (PDP) curves obtained on carbon steel coated with ZnCr (Figure 4a) and ZnNb (Figure 4b) after 1 hour of immersion in a 3.5 wt.% NaCl solution saturated with CO_2 and containing 0.003 M $Na_2S_2O_3.5H_2O$ at 40 °C, and 4 bar CO_2 pressure. Figure 4 shows the anodic and the cathodic polarization curves. For uncoated carbon steel without $S_2O_3^{2-}$ and at more positive potential than the OCP, the measured steady state current density originated from the anodic reaction (dissolution of iron, Equation 1). At more negative potential than the OCP, the measured steady state current density originated from the cathodic reaction (hydrogen evolution via reduction of H^+ (Equation 2) and water molecule). The protons H^+ were generated from the CO_2 dissolved in water (Equation 3) and dissociation of carbonic acid (Equation 4, 5) [27, 28]. If the saturation level of the solution is above 1 (supersaturation), iron and carbonate ions will react, and iron carbonate will precipitate (Equation 6). The iron carbonate layer formed on the steel surface acts as a physical barrier against corrosion by blocking the diffusion of corrosive species to the surface.

$$Fe \Leftrightarrow Fe^{2+} + 2\,e^- \qquad \text{(Equation 1)}$$

$$2\,H^+ + 2\,e^- \Leftrightarrow H_2 \qquad \text{(Equation 2)}$$

$$CO_2 + H_2O \Leftrightarrow H_2CO_3 \qquad \text{(Equation 3)}$$

$$H_2CO_3 \Leftrightarrow HCO_3^- + H^+ \qquad \text{(Equation 4)}$$

$$HCO_3^- \Leftrightarrow CO_3^{2-} + H^+ \qquad \text{(Equation 5)}$$

$$CO_3^{2-} + Fe^{2+} \Leftrightarrow FeCO_3 \qquad \text{(Equation 6)}$$

For coated carbon steel with ZnCr (Figure 4a) and ZnNb (Figure 4b), without $S_2O_3^{2-}$ and at more positive potential than the OCP, the measured steady state current density originated from dissolution of zinc (Equation 7). At more negative potential than the OCP, hydrogen evolution via reduction of H^+ (Equation 2) and water molecule occurs.

$$Zn \Leftrightarrow Zn^{2+} + 2\ e^- \qquad \text{(Equation 7)}$$

If the solution is supersaturated zinc and carbonate ions will react, and zinc carbonate will precipitate (Equation 8). The zinc carbonate layer formed on the steel surface acts as a physical barrier against corrosion by blocking the diffusion of corrosive species to the surface.

$$CO_3^{2-} + Zn^{2+} \Leftrightarrow ZnCO_3 \qquad \text{(Equation 8)}$$

In the presence of $S_2O_3^{2-}$, for uncoated carbon steel and, at more positive potential than the OCP, the anodic curve represents the dissolution of iron (Equation 1). At more negative potential than the OCP, the cathodic curve represents hydrogen evolution via reduction of H^+ (Equation 2) and water molecule and sulfur reduction. In the acid environment and in contact with carbon steel, $S_2O_3^{2-}$ reduced to elemental S according to the following reaction [22]:

$$S_2O_3^{2-} + 6\ H^+ + 4\ e^- \Leftrightarrow 2S^0 + 3\ H_2S \qquad \text{(Equation 9)}$$

$$S_2O_3^{2-} + H^+ + 4\ e^- \Leftrightarrow S^0 + HSO_3^- \qquad \text{(Equation 10)}$$

The elemental sulfur produced by Equations 9 and 10 can further reduce or disproportionate to yield H_2S. Iron can react with elemental sulfur to form FeS [21, 22].

$$4\ S^0 + H_2O + H^+ \Leftrightarrow 3\ H^+ + SO_4^{2-} + 3\ H_2S \qquad \text{(Equation 11)}$$

$$S + 2\ H^+ + 2\ e^- \Leftrightarrow H_2S \qquad \text{(Equation 12)}$$

In the presence of $S_2O_3^{2-}$, for coated carbon steel with ZnCr and ZnNb and at more positive potential than the OCP, the anodic curve represents the dissolution of Zn (Equation 7). At more negative potential than the OCP, the cathodic curve represents hydrogen evolution via reduction of H^+ and water molecule and sulfur reduction (Equation 2 and Equations 9-10). The elemental sulfur produced by Equations 11 and 12 can further reduce or disproportionate to yield H_2S. Zn in contact with hydrogen sulfide and sulfur compounds may develop a film of ZnS which can affect corrosion behavior of Zn coatings [29]. Several studies have shown formation of ZnS from aqueous solution containing thiosulfate and Zn cations [23, 30, 31]. Fathy et al. [31] deposited electrochemically ZnS from aqueous solution containing 0.005 M $Na_2S_2O_3$, 0.003 M Zn^{2+}, and at pH 3 by applying a range of cathodic potentials. The author found that the potential to grow thin and adherent film of ZnS appears to be around is −1.2V. vs. SEC.

For carbon steel coated with ZnCr or ZnNb, the presence of 0.003 M $Na_2S_2O_3.5H_2O$ shifted the corrosion potential to more anodic potential and increased the corrosion current density (Table 3). The corrosion kinetic parameters E_{corr}, i_{corr}, and CR for uncoated and coated carbon steel with Zn cold spray coatings are shown in Table 3. The tested coatings showed similar behavior after 1 hour of exposure in the CO_2/H_2S environment, which indicates that similar electrochemical reactions are taking place on ZnNb and ZnCr. This result also shows that the Zn cold spray coating provides a cathodic protection for carbon steel UNS G10180 with and without thiosulfate.

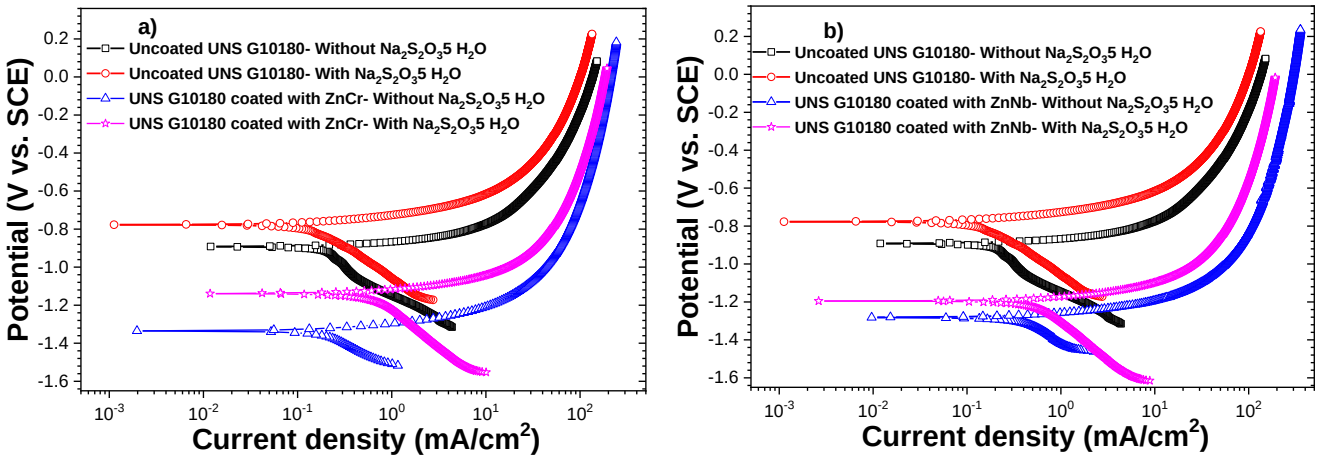

Figure 4: Potentiodynamic polarization curve obtained on uncoated and coated carbon steel with cold spray coatings immersed in a 3.5 wt.% NaCl solution saturated with CO_2 at 40 °C, and 4 bar CO_2 pressure. a). UNS G10180 coated with ZnCr. b). UNS G10180 coated with ZnNb.

Table 3. Corrosion Kinetic Parameters E_{corr}, i_{corr}, and CR for the UNS G10180 and Carbon Steel Coated with Cold Spray Coatings Immersed in a 3.5 wt% NaCl Solution Saturated with CO_2 at 40 °C and 4 bar CO_2 Pressure with and Without $Na_2S_2O_3.5H_2O$

Alloys	E_{corr} (V vs.SCE)	i_{corr} (A/m^2)	β_a (V/decade)	β_c (V/decade)	CR (mm/y)
UNS G10180 - Without $Na_2S_2O_3$ 5H_2O	-0.81± 0.07	1.56 ± 0.02	0.049 ± 0.004	0.223 ± 0.001	1.81 ± 0.02
UNS G10180 - With $Na_2S_2O_3$ 5H_2O	-0.78 ± 0.001	1.2 ± 0.3	0.059 ± 0.01	0.207 ± 0.004	1.39 ± 0.1
UNS G10180 coated with ZnCr - Without $Na_2S_2O_3$ 5H_2O	-1.20 ± 0.07	1.41 ± 0.1	0.052 ± 0.006	0.260 ± 0.006	1.90 ± 0.1
UNS G10180 coated with ZnCr - With $Na_2S_2O_3$ 5H_2O	-1.1 ± 0.01	4.9 ± 0.07	0.055 ± 0.001	0.288 ± 0.007	6.57 ± 0.08
UNS G10180 coated with ZnNb - Without $Na_2S_2O_3$ 5H_2O	-1.26 ± 0.03	3.21 ± 0.08	0.05± 0.003	0.261 ± 0.008	4.77± 0.09
UNS G10180 coated with ZnNb - With $Na_2S_2O_3$ 5H_2O	-1.2 ± 0.06	5.94 ± 0.03	0.056 ± 0.003	0.388 ± 0.007	8.84 ± 0.05

Linear Polarization Resistance Corrosion Rate

The LPR and OCP measurements were conducted to investigate the evolution of corrosion behavior of uncoated and coated carbon steel after 24 hours of immersion in 3.5% NaCl solution. The variation of the OCP and R_p with time for uncoated and coated carbon steel is shown in Figure 5a and Figure 5b, respectively. For uncoated and coated steel, the OCP (Figure 5a) followed a similar trend with and without thiosulfate. However, the OCP shifted to more anodic potential in the presence of thiosulfate. For uncoated and coated carbon steel with cold spray coating and without thiosulfate revealed a higher R_p (Figure 5b) compared to condition with thiosulfate. The increase in OCP and decrease in R_p could be

explained by formation of corrosion product layer iron oxides, iron carbonate, iron sulfide on top of uncoated steel and ZnO, $ZnCO_3$, and ZnS and on top of zinc coatings, which protect carbon steel against CO_2/H_2S corrosion. Under condition without thiosulfate, the main cathodic reaction is a reduction of H^+ and evolution of H_2 (Equation 2) and the main anodic process is the dissolution of iron to Fe^{2+} (Equation 1) and zinc to Zn^{2+} (Equation 7). Under conditions with thiosulfate, at the OCP, the anodic reaction for dissolution of iron or zinc were maintained the same. However, as it was explained in the previous section, the cathodic reactions are hydrogen evolution via reduction of H^+ (Equation 2) and sulfur reduction (Equation 9 to 12). Considering that the electrochemical process at OCP and at these tested conditions was controlled by charge transfer, the corrosion rate is calculated using Equations 1 and 2. The corrosion rate of carbon steel coated with the Zn cold spray coating with and without thiosulfate was higher compared to uncoated UNS G10180 substrate (Figure 6). This is due to cathodic protection of Zn cold spray coatings to the steel. The decrease of corrosion rate for uncoated and coated steel exposed to electrolyte containing thiosulfate may be explained by the notion of an inhibition of the anodic dissolution reaction by the formation of an iron sulfide or zinc sulfide film. This is in good agreement with the literature [9, 10].

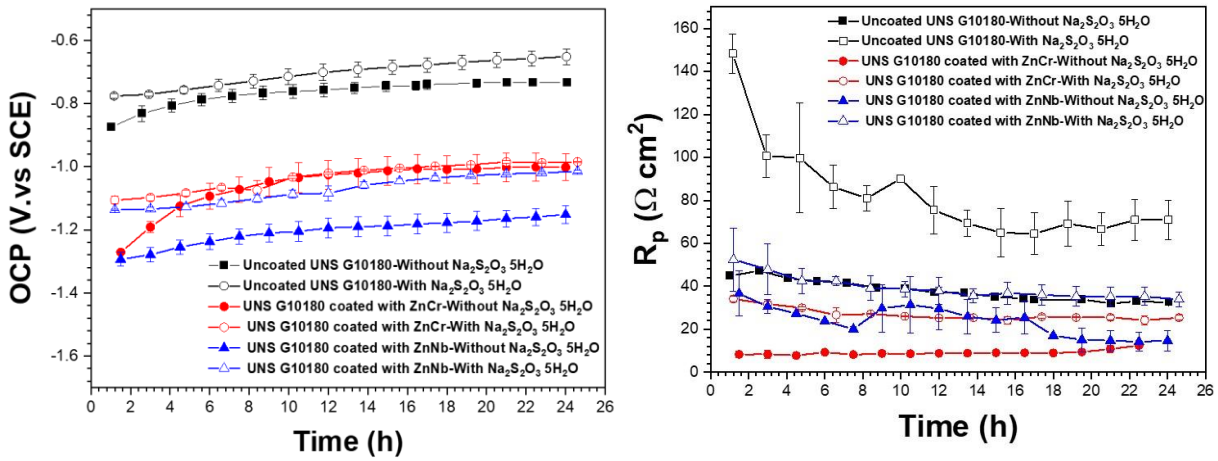

Figure 5: OCP and R_p as a function of time of the Al alloys and carbon steel coated with thermal spray coatings immersed in a 3.5 wt.% NaCl solution saturated with CO_2 at 40 °C and 4 bar CO_2 pressure.

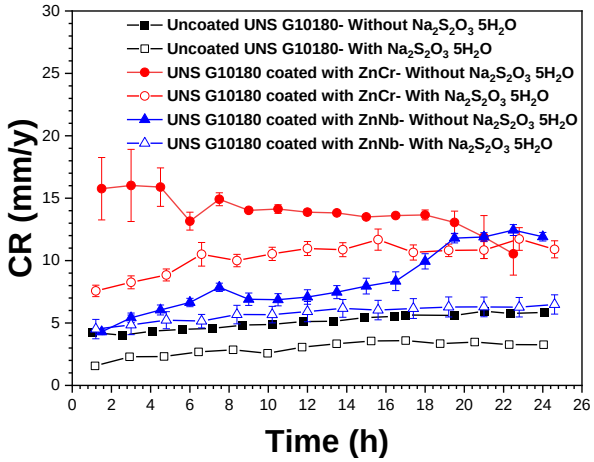

Figure 6: Corrosion rate as a function of time of the Al alloys and carbon steel coated with thermal spray coatings immersed in a 3.5 wt.% NaCl solution saturated with CO_2 at 40 °C and 4 bar CO_2 pressure.

Electrochemical Impedance Spectroscopy

EIS measurements were performed to complement the LPR results. Figure 7 shows the Nyquist plots of uncoated and coated carbon steel with cold spray coatings (ZnCr and ZnNb) after 24 hours of exposure to 3.5 wt.% NaCl solution containing thiosulfate and saturated with 4 bar CO_2 at 40 °C. All impedance spectra showed a depressed capacitive loop at high frequencies indicating a double-layer capacitance. Depressed semi-circles are characteristic for heterogeneous surface roughness and the non-uniform distribution of current density on the surface [24, 32]. For carbon steel coated with ZnCr or ZnNb, with and without thiosulfate, the low-frequency limit of the impedance decreased compared to uncoated steel, indicating decrease in polarization resistance. This result also showed that the zinc cold spray coating provides a cathodic protection for carbon steel UNS G10180 with and without thiosulfate. In the presence of thiosulfate, at low frequency limit, a higher impedance was measured, indicating a decreased corrosion rate, which suggests the H_2S induced inhibition against the CO_2 corrosion of uncoated and coated carbon steel with cold spray coating. In addition to the charge transfer process and the double layer capacitance, a diffusion was observed in the low-frequency domain. This can be attributed to the diffusion of the species through the corrosion product layer. The impedance results confirm the conclusion obtained from potentiodynamic curves and LPR.

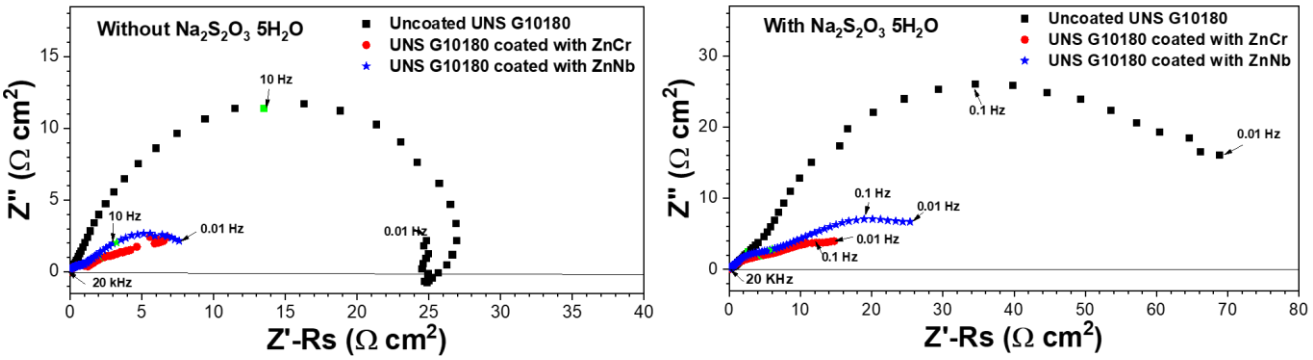

Figure 7: Nyquist diagrams (a) and Bode diagrams (b, c) of Al alloys and carbon steel coated with thermal spray coatings immersed in a 3.5 wt.% NaCl solution saturated with 4 bar CO_2 at 40 °C, after 24 hours.

Surface Characterization

To identify corrosion deposits formed on uncoated UNS G10180 and on top of the coatings (ZnCr and ZnNb), the SEM, EDS, and XRD surface analyses were performed on specimens retrieved after 24 hours exposure to 3.5 wt.% NaCl solution with and without sodium thiosulfate. Figure 8 and Figure 9 show the SEM morphologies before and after exposure and EDS surface analyses for specimens collected at the end of the corrosion test, respectively. For uncoated and coated carbon steel, with and without thiosulfate, general corrosion was apparent and the scratch marks resulting from specimen polishing disappeared after 24 hours of exposure to the 3.5 wt.% NaCl electrolyte. A significant difference was observed in the surface morphology (Figure 8) and in surface chemical composition (Figure 9) before and after 24 hours of exposure to NaCl solution with and without thiosulfate, which all showed indications that there is formation of different types of corrosion products on the surface. For uncoated carbon steel and without thiosulfate, EDS analysis (Figure 9) showed that mainly Fe, C, and O were detected on these steel

surfaces, suggesting the formation of iron oxide and iron carbonate. However, for uncoated steel exposed to NaCl containing thiosulfate, in addition to Fe, C, O, S was detected suggesting formation of iron oxide, iron carbonate, and iron sulfide layers. For coated carbon steel with ZnCr or ZnNb exposed to NaCl containing thiosulfate, EDS mapping analysis of the surface (Figures 9) detected the presence of Zn, C, O, and S in addition to main elements of ZnCr and ZnNb, which suggested the presence of zinc oxides, zinc sulfide, and zinc carbonate layers. In addition, EDS analysis of the carbon steel coated with cold spay coatings, exposed to NaCl with and without thiosulfate, revealed no presence of Fe which confirmed that the steel surface was cathodically protected through a sacrificial anode system (ZnCr or ZnNb). The presence of Cr and Nb elements in Zn cold spray coatings increases corrosion resistance of zinc coatings by accelerating formation of $ZnCO_3$ layer on top of ZnNb and ZnCr coatings. This could be due to galvanic coupling between Zn and Cr or Nb [18, 20].

To identify the composition of the corrosion product layer, XRD analyses were performed on the surface of the specimens with and without thiosulfate. Figure 10 provides a comparison of the XRD pattern of uncoated and coated steel with zinc cold spay coatings before and after 24 hours of immersion in a 3.5 wt.% NaCl solution with and without thiosulfate. For uncoated UNS G10180 and without thiosulfate, the corrosion product was mainly composed of base metal, iron oxides, and iron carbonate (Figure 10). However, in the presence of thiosulfate iron sulfide (mackinawite) was detected. For UNS G10180 coated with cold spray ZnCr or ZnNb, the XRD spectra showed the presence of ZnO $ZnCO_3$. For UNS G10180 coated with cold spray ZnCr and ZnNb exposed to electrolyte containing thiosulfate, the main corrosion product was identified as ZnO, $ZnCO_3$, and ZnS, in addition to the base metal ZnCr or ZnNb. These results are consistent with the EDS analysis.

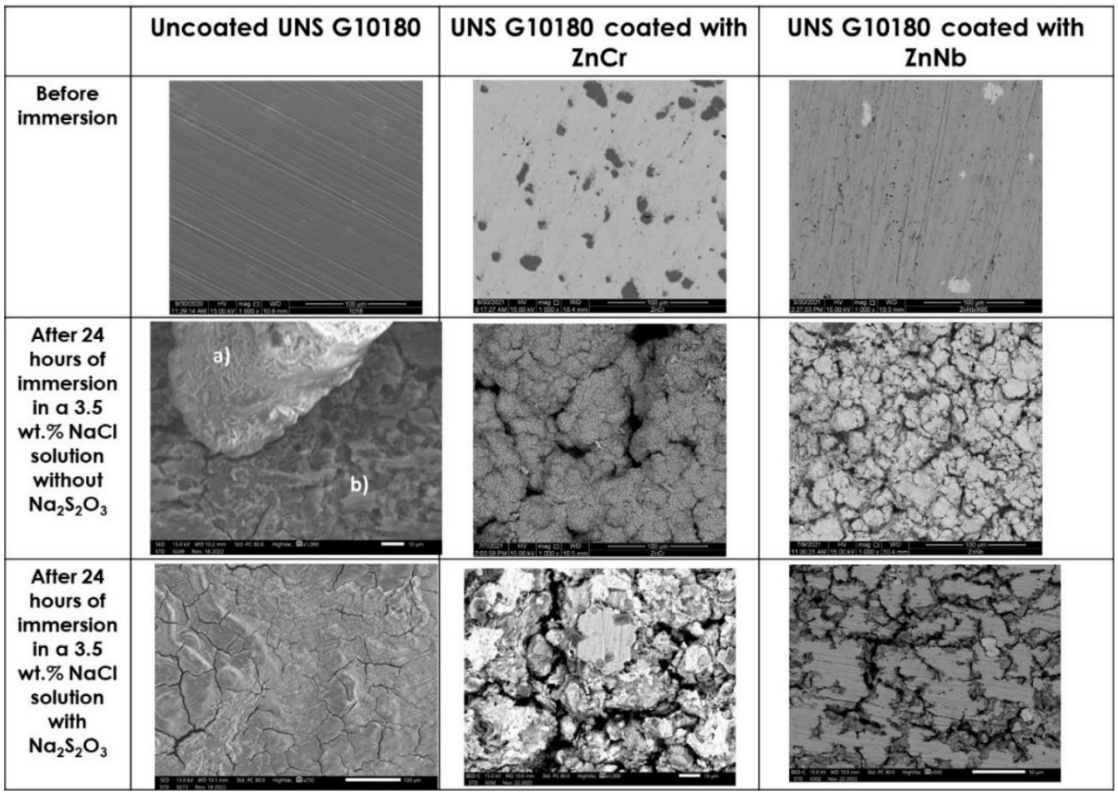

Figure 8: Surface morphology of uncoated and coated steel before and after 24 hours of immersion in a 3.5 wt.% NaCl solution with and without thiosulfate.

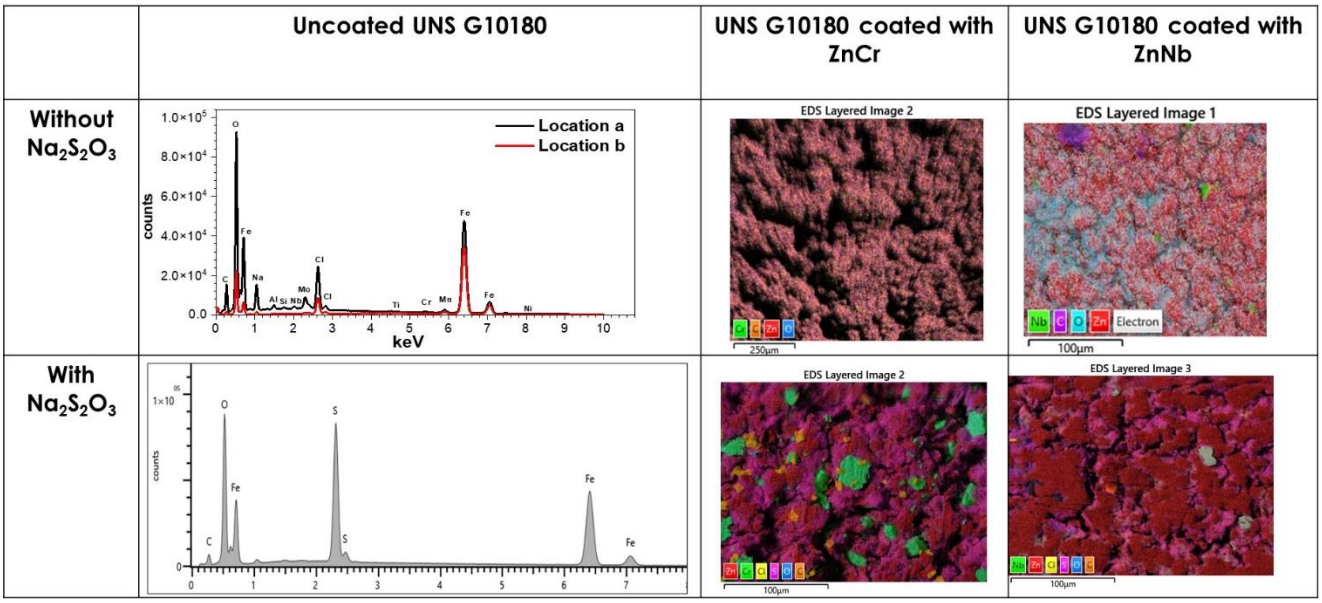

Figure 9: EDS surface analysis of uncoated and coated steel after 24 hours of immersion in a 3.5 wt.% NaCl solution with and without thiosulfate.

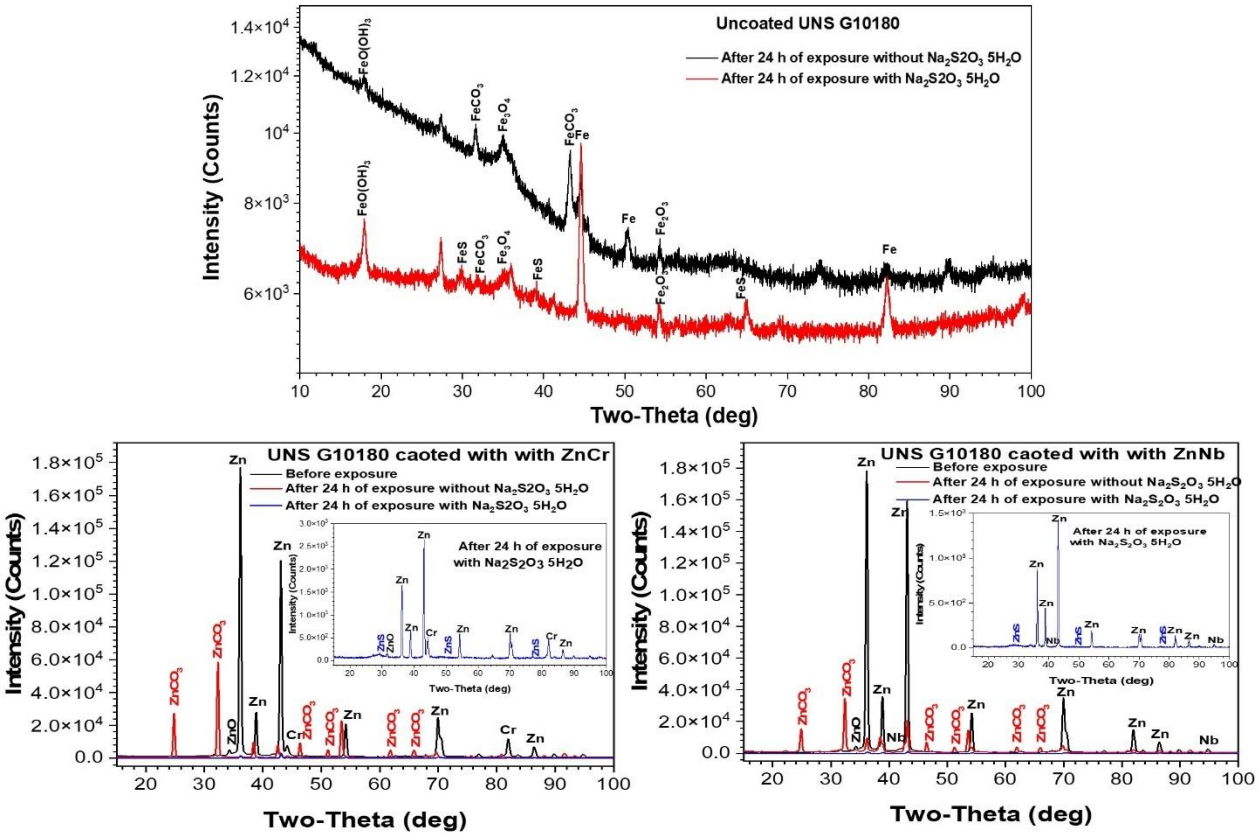

Figure 10. XRD surface analysis of uncoated and coated steel after 24 hours of immersion in a 3.5 wt.% NaCl solution with and without thiosulfate.

To determine the distribution of elements in the metallic coatings and investigate the presence of localized corrosion within and under the metallic coatings, backscattered SEM micrographs and EDS mapping were performed on the cross-section of the specimens after 24 hours exposure to NaCl solution with and without thiosulfate. For uncoated UNS G10180 without thiosulfate, EDS cross-section analysis (Figure 11) detected Fe, O, and C which suggested the likely presence of an iron carbonate layer as an inner layer. However, in the presence of thiosulfate in addition to the iron oxide and iron carbonate, iron sulfide as an outer layer was detected. For carbon steel coated with ZnCr, the corrosion film formed in the absence of thiosulfate is thicker than the corrosion product layer formed on uncoated or coated steel with ZnNb. with thiosulfate. The formation of ZnO, $ZnCO_3$, or ZnS protects ZnCr and ZnNb against corrosion. No localized corrosion has been observed under or within cold spray coating (ZnCr and ZnNb).

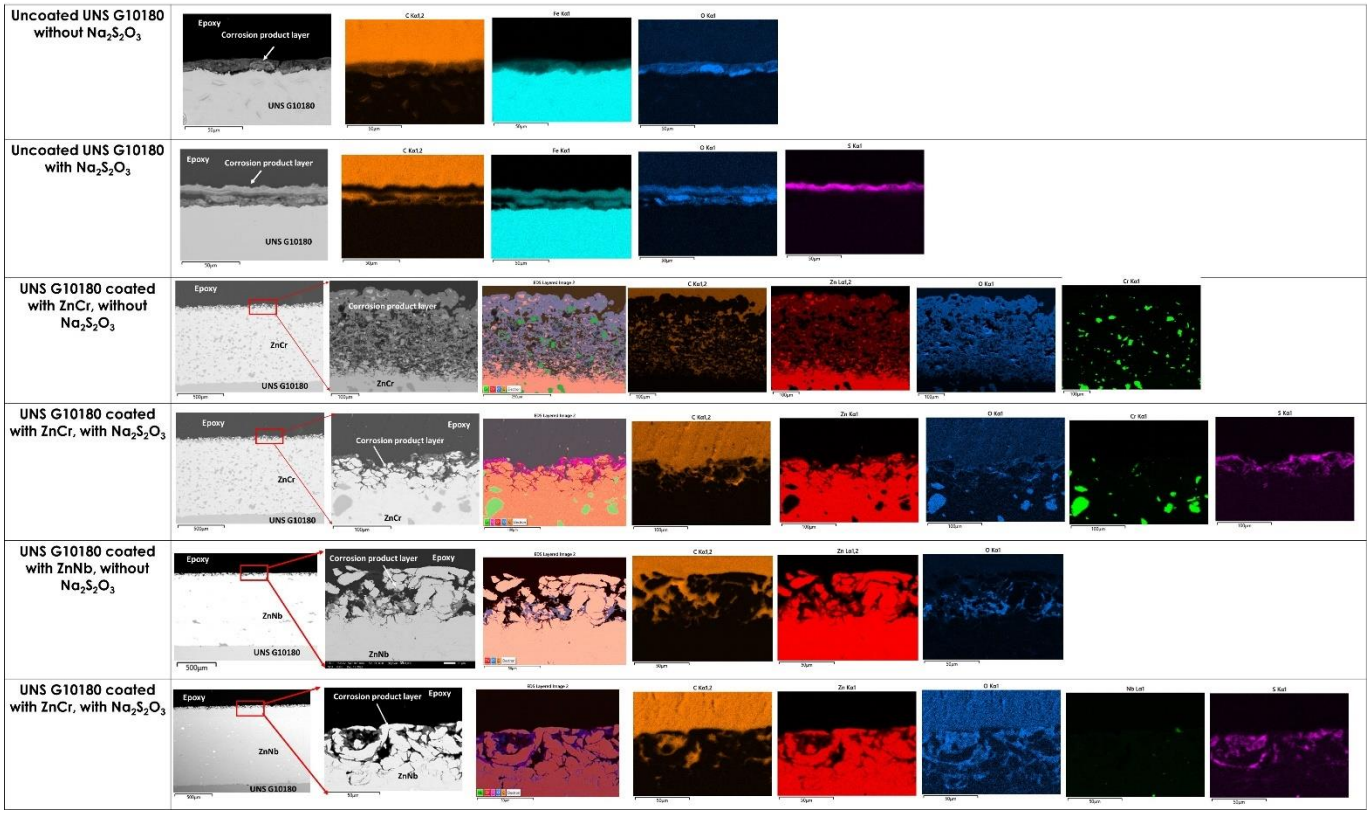

Figure 11: Cross-section SEM and EDS surface mapping of uncoated and coated UNS G10180 with metallic coatings after 24 hours of immersion in a 3.5 wt.% NaCl solution with and without thiosulfate.

CONCLUSIONS

Investigations of the corrosion behavior of carbon steel coated with cold spray coatings (ZnCr and ZnNb) immersed in 3.5 wt.% NaCl solution saturated with CO_2 containing thiosulfate, at 40 °C and, 4 bar CO_2 pressure were performed through several electrochemical methods including potentiodynamic polarization, LPR, and EIS, followed by SEM/EDS characterization of the corrosion products. The main conclusions from this research are:

- Zinc cold spray coatings (ZnCr and ZnNb) provide corrosion protection of carbon steel exposed to simulated wet natural gas with and without thiosulfate.
- The formation of the $ZnCO_3$ layer on top of ZnNb and ZnCr coatings without thiosulfate and ZnS with thiosulfate led to passivation of the coatings which helps to reduce the self-corrosion. These layers form a barrier for diffusion of corrosive species to the surface.
- Under the conditions tested, no localized corrosion was observed on the surface of the cold spray coatings, ZnCr and ZnNb.

ACKNOWLEDGEMENTS

This work was performed in support of the U.S. Department of Energy's (DOE) Office of Fossil Energy and Carbon Management's Methane Mitigation Technologies Program and executed through the National Energy Technology Laboratory (NETL) Research & Innovation Center's Natural Gas Infrastructure FWP. The authors would like to thank Mr. Trevor Godell for machining the corrosion samples and Mr. Jeffrey Oberfoell for his help in the electrochemical autoclave setup. The authors are grateful to Parr Instrument company for providing the autoclave drawing.

DISCLAIMER

REFERENCES

[1] B. J. Berkowitz and H. H. Horowit, "The role of H_2S in the corrosion and hydrogen embrittlement of steel," *Journal of The Electrochemical Society,* vol. 129, no. 3, p. 468, 1982.

[2] M. B. Kermani, "Materials optimization for oil and gas sour production," in *CORROSION/2000, Paper No. 156 (Houston Tx; NACE, 2000).* .

[3] Y. Gunaltun and D. Larrey, " Correlation of cases of top-of-the-line corrosion with calculated water condensation rates," CORROSION/2000, Paper No. 71 (Houston Tx; NACE, 2000).

[4] E. C. Greco and W. B. Wright, " Corrosion of Iron in an H_2S-CO_2-H_2O System," *Corrosion ,* vol. 18, pp. 119-124, 1962.

[5] J. Sardisco, W. Wright and E. Greco, "Corrosion of iron in on H_2S-CO_2-H_2O system: corrosion film properties on pure iron," *Corrosion,* vol. 19, no. 10, pp. 354t-359t, 1963.

[6] J. B. Sardisco and R. E. Pitts, "Corrosion of iron in an H_2S-CO_2-H_2O system mechanism of sulfide film formation and kinetics of corrosion reaction," *Corrosion,* vol. 21, no. 8, pp. 245-253, 1965.

[7] H. Maa, X. Cheng, G. Li, S. Chen, Z. Quan, S. Zhao and L. Niu, "The in¯uence of hydrogen sul®de on corrosion of iron under diffrent conditions," *Corrosion Science,* vol. 42, pp. 1669-1683, 2000.

[8] S. N. Esmaeely, B. Brown and S. Nesic, "Verification of an electrochemical model for aqueous corrosion of mild steel for H_2S partial pressures up to 0.1 MP," *Corrosion,* vol. 73, no. 2, pp. 144-154, 2017.

[9] W. Sun, S. Nesic and S. Papavinasam, "Kinetics of corrosion layer formation: Part 2—iron sulfide and mixed iron sulfide/carbonate layers in carbon dioxide/hydrogen sulfide corrosion corrosion," *Corrosion,* vol. 64, no. 7, pp. 586-599, 2008.

[10] Y.-S. Choi, S. Nesic and S. Ling, " Effect of H_2S on the CO_2 corrosion of carbon steel in acidic solutions," *Electrochimica Acta ,* vol. 56 , p. 1752–1760, 2011.

[11] T. E. Perez, "Corrosion in the oil and gas industry: An Increasing challenge for materials," *The Journal of The Minerals, Metals & Materials Society (TMS),* vol. 65, no. 8, pp. 1033-1042, 2013.

[12] N. M. 15156, " Petroleum and Natural Gas Industries—Materials for Use in H2S-Containing Environments in Oil and Gas Production," in *(Houston, TX: NACE, 2003)*, (2009).

[13] M. Iannuzzi and D. N. Verita, "Environmentally assisted cracking (EAC) in oil and gas production," in *Stress Corrosion Cracking Theory and Practice* , Woodhead Publishing in Metals and Surface Engineering , 2011, pp. 570-607.

[14] C. Xie, H. Li, X. Zhou and C. Sun, "Corrosion behavior of cold sprayed pure zinc coating on magnesium," *Surface & Coatings Technology ,* vol. 374, p. 797–806, 374 (2019) -26,27.

[15] Q. Jianga, Q. Miao, W. Liang, F. Ying, F. Tong, Y. Xu, B. L. Ren and P. Z. Z. J. Yao, "Corrosion behavior of arc sprayed Al–Zn–Si–RE coatings on mild steel in 3.5 wt% NaCl solution," *Electrochemical Acta,* vol. 115, pp. 644-656, 2014.

[16] N. M. Chavan, B. Kiran, A. Jyothirmayi, P. S. Phani and G. Sundararajan, "The Corrosion Behavior of Cold Sprayed Zinc Coatings on Mild Steel Substrate," *Journal of Thermal Spray Technology volume,* vol. 22, pp. 463-470, 2013.

[17] L. Teeter, M. Ziomek-Moroz, J. Tylczak and G. Crawford, "ZnCr and ZnNb Cold Spray Coatings," in *NACE, CORROSION 2021*, Houston, TX, 2021.

[18] Z. Belarbi, L. Teeter, R. Chinn and O. Dogan, "Binary Sacrificial Coatings for Internal Corrosion Protection of Natural Gas Transmission Pipelines,," in *ECS Meeting Abstracts MA2022-01-0686.* , 2022.

[19] L. Teeter, M. Z.-. Moroz, J. Tylczak and G. Crawford, " ZnCr and ZnNb Cold Spray Coatings;," in *CORROSION 2021, paper no 16977 (NACE-2021)*.

[20] Z. Belarbi, R. E. Chinn, O. Dogan, P. Carr and J. Samson, " Field Testing of Self-Healing Metallic Coatings for Internal Corrosion Protection of Natural Gas Pipelines," in *AMPP 2023, paper no 18857 (AMPP, 2023)*.

[21] S. Tsujikawa, A. Miyasaka, M. Ueda, S. Ando, T. Shibata, T. Haruna, M. Katahira, Y. Yamane, T. Aoki and T. Yamada, "Alternative for evaluating sour gas resistance of low-alloy steels and corrosion-resistant alloys," *Corrosion,* vol. 49, no. 5, pp. 409-419, 1993.

[22] M. Kappes, G. S. Frankel, N. Sridhar and R. M. Carranza, " Reaction paths of tiosulfate during corrosion of carbon steel in acidified brines," *Journal of The Electrochemical Society,,* vol. 159, no. 4, pp. C195-C204, 2012.

[23] I. V. Demidenko and V. M. Ishimov, "Electrochemical deposition of zinc sulfide from a Na_2SO_3-based electrolyte," *Surface Engineering and Applied Electrochemistry,* vol. 58, pp. 109-115, 2022.

[24] Z. Belarbi, J. Tylczak and M. Ziomek-Moroz, "Mitigating CO_2 corrosion of natural gas steel pipelines by thermal spray aluminum coatings," *Corrosion,* vol. 48, no. 1, pp. 68-86, 2022.

[25] F. Mansfeld and K. B. Oldham, "A modification of the Stern—Geary linear polarization equation," *Corrosion Science ,* vol. 11, no. 10, p. 787, 1971.

[26] R. Feng, J. Beck, M. Ziomek-Moroz and S. N. Lvov, "Electrochemical corrosion of ultra-high strength carbon steel in alkaline brines containing hydrogen sulfide," *Electrochimica Acta ,* vol. 212, no. 10, p. 998, 2016.

[27] A. Kahyarian and S. Nesic, " On the mechanism of carbon dioxide corrosion of mild steel: Experimental investigation and mathematical modeling at elevated pressures and non-ideal solutions," *Corrosion Science,* vol. 173, p. 108719, 2020.

[28] S. Nesic, "Key issues related to modelling of internal corrosion of oil and gas pipelines – A review," *Corrosion Science ,* vol. 49, p. 4308–4338, 2007.

[29] N. Arbi, I. B. Assaker, M. Gannouni, A. Kriaa and R. Chtourou, "Experimental investigation of the effect of Zn/S molar ratios on the physical and electrochemcial properietis of znS thin film," *Materials Science in Semiconductor Processing,* vol. 40, pp. 873-878, 2015.

[30] N. Fathy, R. Kobayashi and M. Ichimura, "Preparation of ZnS thin films by the pulsed electrochemical deposition," *Materials Science and Engineering,* vol. B107, pp. 271-276, 2004.

[31] N. Fathy and M. Ichimura, "Photoelectrical properties of ZnS thin films depositited from aquous solution using pulsed electrochemical deposition," *Solar Energy Materials & Solar Cells,* vol. 87, pp. 747-756, 2005.

[32] Z. Belarbi, F. Farelas, M. Singer and S. Nesic, "Role of amines in the mitigation of CO_2 Top of the Line Corrosion," *Corrosion,* vol. 72, no. 10, p. 1300, 2016.